Stability of Absorbing Boundary Conditions

Omar M. Ramahi, *Member, IEEE*

***Abstract*— Higher order absorbing boundary conditions (ABC's) exhibit instabilities that can be detrimental to a wide class of finite-difference time-domain (FDTD) open-region simulations. Earlier works attributed the cause of instabilities to the intrinsic construction or makeup of the ABC's, and consequently to the pole-zero distribution of the transfer function that characterizes the boundary condition. In this work, we investigate the cause of instability. We focus on axial boundary conditions such as Higdon, Bayliss–Turkel, and Liao, and show through an empirical study that these ABC's are not intrinsically unstable in their original unmodified forms. Furthermore, we show that the instability typically observed in FDTD open-region simulations is caused by an artifact of the rectangular computational domain, contrary to previously conjectured hypotheses or theories. These findings will have strong implications that can aid in the construction of stable FDTD schemes.**

***Index Terms*—Absorbing boundary conditions, finite-difference time-domain method, stability.**

I. Introduction

WHENEVER the finite-difference time-domain (FDTD) method is used to simulate open-region radiation or scattering problems, the implementation of a mesh-truncation scheme becomes an integral part of the simulation. For many FDTD applications, the required duration of the simulation need only to extend over enough time steps to capture the bulk of the output energy or pulse at a desired point of observation. For such problems, the stability behavior of mesh-truncation techniques does not pose a serious challenge. However, there is a wide class of problems where the output time signature needs to be obtained for a very long duration in order to reproduce the response of the system over a wide frequency band (via Fourier transformation). For this important class of problems, care must be taken to ensure that the evolution of the field in time does not exhibit any unstable behavior.

In the electromagnetic computational context, instability is generally referred to the time-dependent growth of the solution such that it violates the physical phenomenon being simulated. The potential of the solution to become unstable is a concern not only when using the FDTD method, but whenever a time-domain technique is encountered such as the time-domain method of moments (MoM) and the time-domain finite elements method (FEM). (See [1] and [2] and references therein for a perspective on the importance of the subject of stability in MoM and FEM.) When the growth in time of the solution is slow or weak in comparison to the maximum peak of the signal, the instability is commonly referred to as late-time instability. Unfortunately, such nomenclature can be misleading since the degree of growth of the solution should be measured with respect to, or in relation to the frequency bandwidth of the analysis. For instance, when one is interested only in the response of the system over a narrow band of frequency, then what is referred to as late-time instability can be of little concern. However, when the interest lies in the behavior of the system over a wide frequency band, then the FDTD simulation would need to include a sufficiently large number of time steps to capture the correct frequency response. In these applications, a small growth in the solution can have a detrimental effect on the lower frequency response. Also, when analyzing open-region resonant structures such as microstrip filters, the simulation needs to proceed for an excessively large number of time steps to capture the resonant frequencies accurately. Again, any artificial growth in the solution renders the simulation useless.

Instabilities in the FDTD method are caused by different mechanisms; some of which are understood and some have remained unresolved. The most visible cause of instability is related to the relationship between the grid spacing and the time step, typically referred to in the electromagnetic literature as the Courant–Friedrichs–Lewy (CFL) criterion. This type of instability is resolved by adhering to the CFL condition. The second important type of instability is caused by the mesh-truncation technique that is essential to produce a finite computational domain when simulating open-region problems. This type of instability arises at the analytical level or at the numerical level. If the mesh-truncation mechanism or the boundary condition is intrinsically ill posed, then the instability is analytical. An ill-posed formulation implies the nonuniqueness of the solution. Alternatively, a well-posed solution does not admit a reflection that can grow in time. The ill posedness of a boundary condition is typically addressed at the formulation stage of the problem and for the most part is of minor concern to practical FDTD modelers.

On the other hand, the instabilities that arise at the numerical level are more difficult to analyze. This is primarily due to the fact that the mapping from the analytical domain to the discrete domain is not unique; thus, each discretization scheme has to be carefully scrutinized for its instability potential.

Mesh-truncation techniques fall into two distinct categories: The first consists of material-based techniques, and the second of absorbing boundary condition (ABC)-based techniques. In the first group, the perfectly matched layer (PML) figures prominently [3]. Few publications have addressed the subject of PML stability. Recently, it was found that the split version of the PML to be not strongly well posed [4], which merits

Manuscript received March 15, 1998; revised November 23, 1998.

The author is with the Compaq Computer Corporation, Maynard, MA 01754 USA.

Publisher Item Identifier S 0018-926X(99)04789-4.

further investigation in the general stability properties of PML. The second group of mesh-truncation techniques include ABC's such as Bayliss–Turkel [5], Engquist–Majda [6], and Higdon [7], [8], in addition to methods based directly or indirectly on these ABC's such as the class of numerical operators [9], [10], and the complementary operators method (COM) [11], [12]. In this work, we focus on the instability caused by the second group. Furthermore, we concentrate only on ABC's that are uni-axial (involve only normal derivatives in space) such as Bayliss–Turkel, Higdon, and Liao. These ABC's are considered here because of their unique flexibility and ease of construction, but also because of their simple and direct applicability in the COM method. However, it will be seen from the discussion and findings in this work that it is most likely that the conclusions inferred henceforth are applicable to other analytical ABC's.

II. Absorbing Boundary Conditions

It is commonly established that higher order ABC's introduce instabilities into the FDTD simulation of open-region problems. Previous work exhibiting such instabilities dealt primarily with Higdon and Liao ABC's [8], [13], nevertheless, it is highly probable that the stability behavior transcends to other classes of analytical ABC's.

The cause of instability arising from the application of higher-order ABC's has been attributed to at least one of the following factors: 1) finite computer precision; 2) differencing schemes used to approximate the differential boundary operator; and 3) low-frequency content of the excitation pulse. In consequence, several remedies were proposed, some which are simple, such as increasing the computer arithmetic precision in the mesh region of the computational domain occupied by the numerical stencil of the ABC [14]. The numerical stencil, henceforth referred to as the stencil, refers to the nodes that are needed to discretize a given boundary condition. The differencing schemes used to translate an analytic partial differential equation into a discrete algebraic equation are not unique. In fact, the mathematical definition of the derivative does not have to be unique and can be generalized to a wider class as long as the limit behavior remains unchanged ([15] and references therein). Some schemes used within the FDTD method to discretize boundary operators have been found, empirically, to yield satisfactory result [6]. Because of the varying possibilities available to discretize an equation, weighting coefficients can be inserted in addition to different averaging measures [8], which were found to increase the stability potential of certain ABC's. However, it needs to be stressed that, to the author's knowledge, no systematic study has been carried out on this subject, especially the effect of the discretization scheme on stability.

The third factor considered to cause instability has been investigated in the context of Maxwell's equations. When the pulse contains sufficient energy in the lower frequency components (close to dc) it was suggested that the solution employing an ABC becomes unstable because of the increase, above unity, of the reflection coefficient [8]. Let us consider the Nth order Higdon ABC enforced at the left-hand side of a rectangular terminal boundary (parallel to the y-axis). The operator B which represents the ABC and its corresponding analytic reflection coefficient, R, are given, respectively, by

$$B\{u\} = \prod_{i=1}^{N} (\partial_x + \frac{\xi_i}{c}\partial_t)u = 0 \tag{1}$$

$$R(B) = -\prod_{i=1}^{N} \left(\frac{-jk_x + j\xi_i\omega/c}{jk_x + j\xi_i\omega/c} \right) \tag{2}$$

where ξ_i is a constant that can be chosen to maximize the absorption in a specified direction, c is the speed of light in free space, ω is the radian frequency, and k_x is the wave number in the x-direction.

In [8] it was argued that as the frequency approaches dc, the denominator in R approaches zero, thus creating a potential for instability. An alternative explanation of this potential cause of instability can be presented based on the theory of Z-transformation, in which the reflection coefficient is recast in the descretized domain as a transfer function. (In this construction, the transform variable z corresponds to a time shift.) From the theory of discrete signal processing, the system described by the transfer function is stable if the poles of the transfer function lie within the unit circle. Since the boundary condition given in (1) produces poles that lie precisely on the unit circle, the FDTD scheme will be only marginally stable [8]. Any slight shift of the poles outside the unit circle would therefore render the boundary condition unstable. A shift of the poles can be caused by limited computer word length and can be prevented by using higher arithmetic precision [14].

Based on the above analysis, it was suggested in [8], that the instability can be prevented by introducing a loss factor ε_i resulting in a new ABC given by

$$B\{u\} = \prod_{i=1}^{N} (\partial_x + \frac{\xi_i}{c}\partial_t + \varepsilon_i) = 0 \tag{3}$$

with a corresponding reflection coefficient given by

$$R(B) = -\prod_{i=1}^{N} \left(\frac{-jk_x + j\xi_i\omega/c + \varepsilon_i}{jk_x + j\xi_i\omega/c + \varepsilon_i} \right). \tag{4}$$

By observation of (4), we see that the introduction of the frequency independent term ε_i prevents the denominator of $R(B)$ from reaching zero as ω approaches zero. Viewed in the context of Z-transforms, the introduction of ε_i shifts the poles of the transfer function into the interior of the unit circle, thus maintaining stability. What is unfortunate, however, is that the order of the pole increases as the order of the boundary condition [higher N in (3)], and it is expected that the stabilization of the boundary condition becomes more difficult. Another important point is that while the introduction of ε_i increases the stability potential of the ABC, it adversely impacts the frequency domain behavior of the solution over the lower end of the spectrum [14]. This is because the reflection coefficient (4) ceases to be frequency independent when ε_i is introduced, and approaches unity monotonically as the frequency approaches dc.

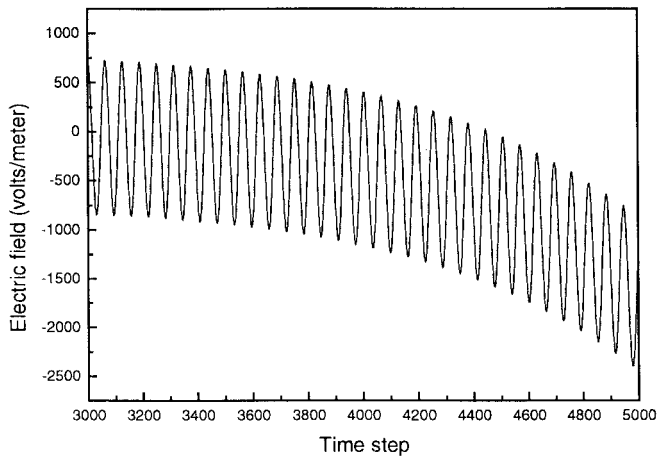

Fig. 1. Solution due to a sinusoidal signal.

This limitation can be significant when the objective of the analysis is the frequency response over a wide-band. For problems requiring the frequency response over a very narrow band, one can always choose a small ε_i sufficient enough to stabilize the solution, yet affecting the accuracy of the solution in a negligible way.

The theory that the lower frequencies are responsible for instabilities can perhaps explain the mechanism of instability; however, it falls short of explaining why the solution can become unstable even when its lower frequency content is virtually null. To expound upon this we consider a source with virtually zero low-frequency content. Throughout this paper, we adopt the following notation: For a domain of size $N\Delta \times M\Delta$, we use $N \times M$. Similarly, an observation point at ($n\Delta$, $m\Delta$) is denoted by (n, m). We consider a 40 $\times$ 40 two-dimensional computational domain where the space step is 0.015 m and the time step is 90% of the CFL limit. The excitation is a line source with a simple sinusoidal temporal waveform positioned at (20, 20) (E- or TM-polarization). The observation point is at (36, 20) Fig. 1 shows the E_z component of the solution obtained using Higdon fourth-order ABC [$N = 4$ in (1)]. Notice that despite the fact that the output pulse has hardly any lower frequency components, the solution still becomes highly unstable. This simple counter example leaves the lower frequencies theory incomplete.

In the strict sense, the "stabilized" forms of Higdon and Liao boundary conditions improved the stability potential of these ABC's, but certainly did not eliminate the instability altogether. Furthermore, efforts to stabilize higher order ABC's were unsuccessful [13]. And when stability is achieved it most likely compromises the solution's accuracy over the lower end of the frequency spectrum [14].

The analyzes advocated initially by Higdon and later used and generalized to Liao's ABC's by Wagner and Chew [13] helped to partially explain the mechanism behind a type of instability. It will be shown in the next section, that the pole-zero distribution of the transfer function can explain only partially the instability mechanism. However, the cause of instability is yet another form of incompatibility that can be also interpreted in light of the analyzes above.

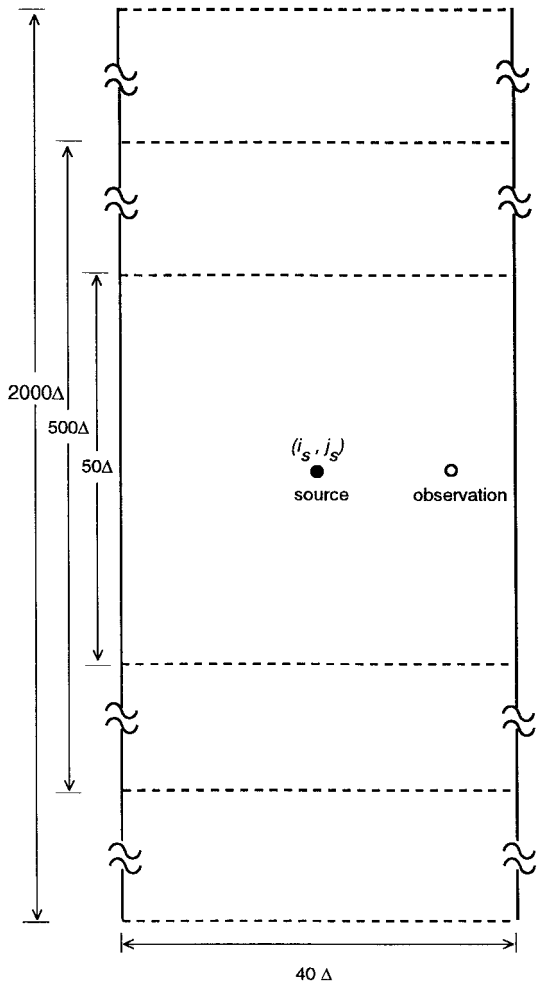

Fig. 2. Computational domains with increasing source-to-corner distance.

III. Isolation of Corner Regions

Let us consider several computational domains in two-dimensional space. The vertical terminal boundaries will be fixed, while the horizontal boundaries (top and bottom) are positioned at different locations to give three different computational domains having sizes 40 $\times$ 50, 40 $\times$ 500, and 40 $\times$ 2000. A diagram illustrating these experimental boundaries is shown in Fig. 2. For each computational domain, the source is positioned at the center of the domain denoted by (i_s, j_s), and the observation point is selected at $((i_s + 18)$, $j_s)$. The excitation is E-polarized with a source having a smooth temporal waveform (resembling a differentiated Gaussian pulse) used in [11]. (In this and the following examples, the precise nature of the pulse waveform is not relevant to the discussion.)

Notice that as the horizontal terminal boundaries (top and bottom) are positioned further away from the source, the distance from the source to the corner regions is increased, while the distance from the source to the observation point remains unchanged at 18 cells. Fig. 3 shows the component of the E_z field at the observation point as calculated in each of the three computational domains. Higdon fourth-order ABC is used without any loss factor $\varepsilon_i = 0$. Observation of

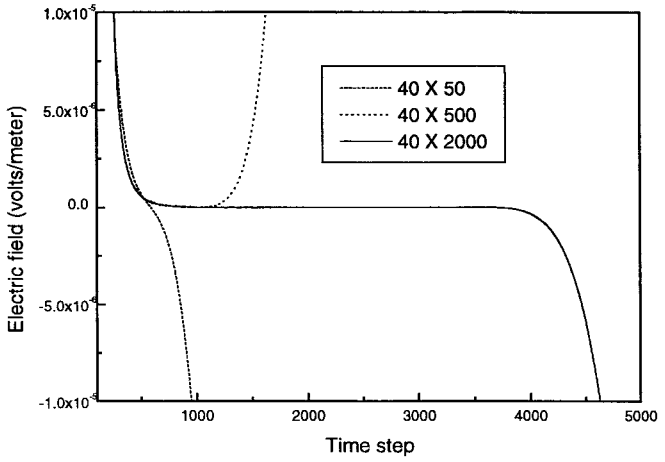

Fig. 3. Instabilities arising from corner regions.

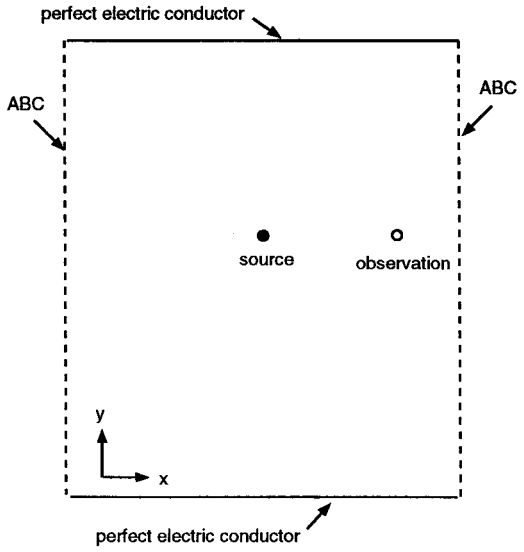

Fig. 4. Computational domain devoid of corner regions.

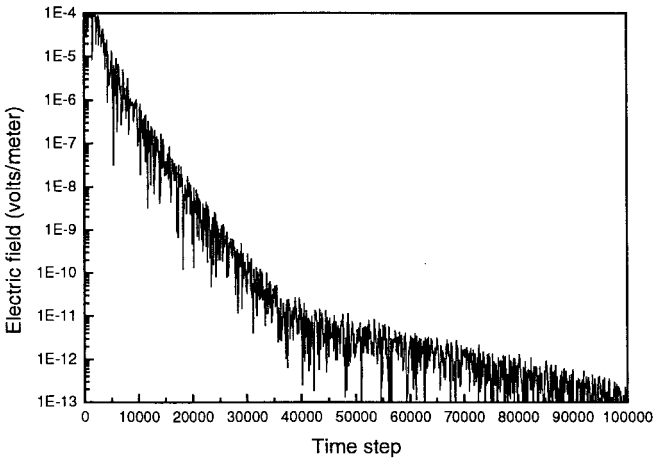

Fig. 5. Solution obtained using Higdon fourth-order ABC.

these curves shows that the solution starts to become unstable precisely as the time waveform reaches the corner region. The start of the instability in Fig. 3 for each curve corresponds to the distance the wavefront takes to travel from the source to the nearest corner region. What is crucial to observe here, is that the "side or vertical boundaries" (which are the closest to the source) did not produce any instability, even though a fourth-order Higdon ABC was used without involving any stabilizing factors. This experiment leads to an important empirical finding; that the instability arise in the corner region and is not caused by the interaction of the wavefront with the side boundaries.

As a further consolidation of this finding, we consider a second numerical experiment in which the effect of the ABC corner regions is eliminated. The most practical way to eliminate the effect of ABC corners and to be able to perform the simulation over large number of time steps is to replace any two parallel boundaries with perfectly conducting plates as shown in Fig. 4. For this problem, the source is a line source polarized in the z-direction (TM polarization) having a temporal waveform and simulation parameters as in the previous example. Fig. 5 shows the FDTD solution obtained for 100 000 time steps while using Higdon fourth-order ABC without any stabilizing parameters. The results presented in Fig. 5 show conclusively that the solution waveform could approach very low values without triggering any instability. Clearly, in the absence of ABC corner regions, the wavefront interacts singularly with the ABC enforced on a side boundary resulting in stable solution.

An important corollary to this finding impacts the simulation of a class of waveguiding structures that have no ABC corner regions such as shown in Fig. 6. In this class of structures, the waveguide geometry ends with planar terminal boundaries defining the FDTD computational domain. Since the FDTD domain is devoid of any corner regions, higher-order ABC's can be employed without concern for instabilities. This corollary has a significant implication in the simulation of dispersive structures such as shielded microstrip lines; especially structures containing resonant discontinuities which demand excessively large number of time steps. As a practical demonstration, we consider a microstrip structure with a cross section in the x–y plane shown in the inset of Fig. 7. The size of the computational domain is $50 \times 40 \times 100$. The source is positioned ten cells from the near-end of the guide and the observation plane (for both current and voltage) is ten cells inward from the far-end terminal boundary. On both terminal boundaries, a fourth-order Higdon ABC is enforced with ξ_1 to ξ_4 having values between one and $\sqrt{\varepsilon_r}$ (the solution is insensitive to variations in ξ_i's as long as they are spread between one and $\sqrt{\varepsilon_r}$). Fig. 7 shows the characteristic impedance calculated from field values obtained from a simulation that ran for 3000 time steps. Comparison is made with the reference solution, which was obtained by considering a long enough guide (350 cells in the z-direction) such that the reflection from the far end does not reach the observation plane. Considering that this structure is highly dispersive, we see that the fourth-order ABC achieved a very satisfactory level of accuracy without resorting to postprocessing or other indirect techniques as would be necessary had we used a lower order ABC [16], [17].

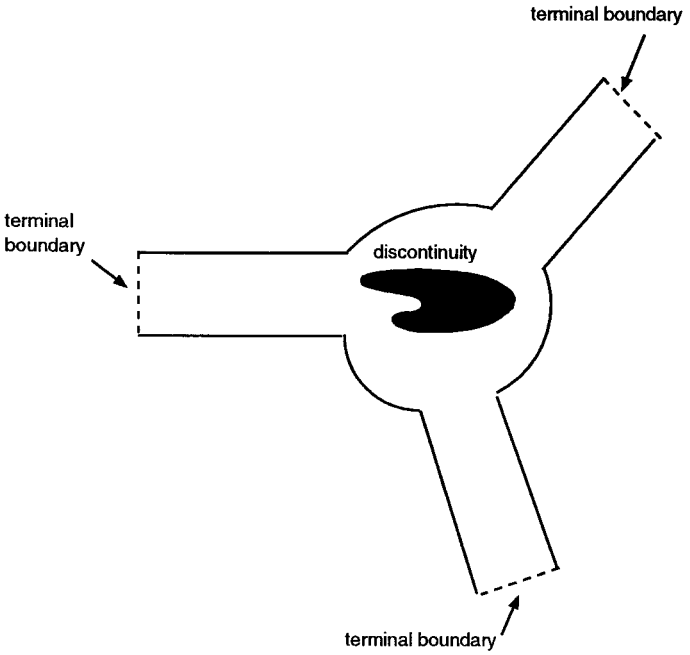

Fig. 6. Geometry for a three-port waveguiding structure showing a discontinuity.

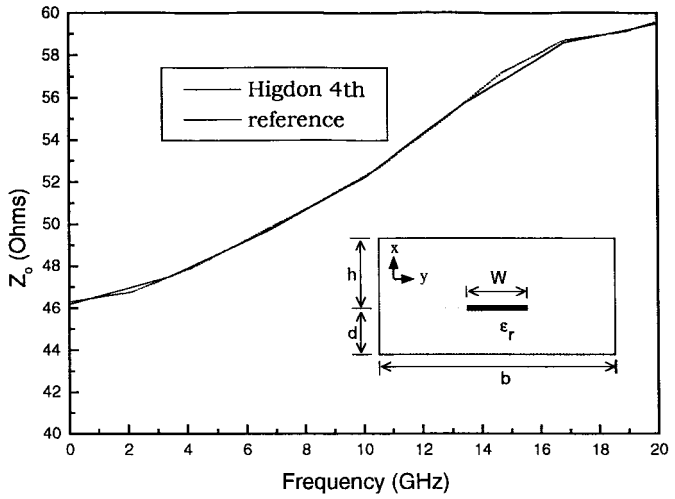

Fig. 7. Characteristic impedance obtained using a domain of size $50 \times 40 \times 100$. Comparison is made with the reference solution devoid of any terminal boundary reflections. $\Delta x = 0.1$ mm, $\Delta y = \Delta z = 0.25$ mm, $h = 4$ mm, $\Delta = 1$ mm, $b = 10$ mm, $W = 1$ mm, $\varepsilon_r = 10$.

Having established that the instability arises in the corner region, it would then be expected that if the outer boundary is a smoothly varying contour, then the instability problem would not arise. To test this hypothesis, we consider the simplest of such contours; a circle. On this, we enforce a fourth-order Bayliss–Turkel ABC [5] given by

$$B\{u\} = \prod_{i=1}^{N} (\partial_\rho + (2i - 3/2)/\rho + \partial_t)u = 0 \qquad (5)$$

where ρ is the radius of the circular contour. The Bayliss–Turkel operators are, in effect, a generalization of Higdon's ABC's. This can be seen as ρ increases, the second term in (5) approaches zero in the limit, thus corresponding

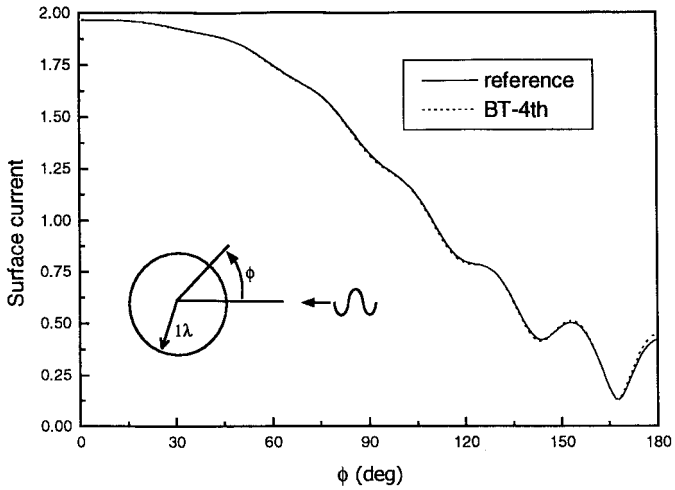

Fig. 8. Surface current on a perfectly conducting circular cylinder due to a TE-polarized plane wave incidence.

to a half-plane terminal boundary. It is important, however, to keep in mind that the second coefficient in (5) is a correction that adjusts for the curvature of the wavefront when expanded on a circular outer boundary and thus it cannot be interpreted to play the role of the loss factor ε_i in (3).

Without loss of generality, we demonstrate the effect of circular outer boundaries on stability by using a recently reported FDTD scheme having an unstaggered mesh ([18] and references therein). We consider the problem of a plane wave (TE-polarization) scattering from a perfectly conducting cylinder with a 1λ radius. The outer boundary is positioned only ten radial cells from the conductor's surface. The mesh consists of 360 cells in the angular direction and ten cells in the radial direction. Fig. 8 shows the surface current obtained using Baylilss–Turkel's fourth-order ABC and the reference solution (obtained through Hankel's function expansion). The surface current was obtained from the total field samples for a simulation spanning 20 000 time steps. What is to be emphasized here is that not only the simulation was free from any instability, but equally important, it resulted in a remarkably accurate solution that can hardly be distinguished from the reference solution.

The above experiments lead us to conclude that higher order ABC's are not intrinsically unstable. Furthermore, the instability arises from an artifact of the computational domain that causes an incompatibility, which we discuss in the following section.

IV. Corner Region Incompatibility

The incompatibility that arises at corner regions is linked to the numerical process that converts the solution process from the analytical to the numerical domain. In the analytic domain, the boundary operator, which is composed of differential operators in time and space, is applied at a single point in space and time. When the analytic operator is converted to a discrete operator through finite-difference approximation, it can no longer be applied at a single point in space and time, but now it is applied over a set of points, or a stencil. This directly leads to the potential incompatibility when encountering points

close to the corner regions and, in other applications, to points close to any terminal boundary. (For instance, in [19], the averaging of the fields that reflect off the terminal boundary must take place at a plane located beyond the stencil region.) The appearance of any sudden irregularity within the stencil region, such as a "source term" creates a discontinuity in the field and its derivatives that compromises the assumption of analyticity of the field in that region. As a consequence, the definition of the partial derivatives, ∂x and ∂t, within the stencil become meaningless (unless the analysis is carried out within the context of the theory of distributions).

To explain this in more detail, recall that boundary conditions are constructed under the assumption that the electromagnetic fields in their proximity satisfy the homogeneous wave equation. This implies that the region over which the ABC is enforced cannot contain sources or virtual discontinuities. Let us consider the upper right-hand corner region in a two-dimensional FDTD. Without loss of generality, we show in Fig. 9 the stencils of a third-order Higdon's ABC. For clarity, we limit this discussion to the two-dimensional space, however the conclusions apply to the three-dimensional space. Let us apply the ABC on node A shown in Fig. 9. Assuming that the incident field has the wave number $\boldsymbol{k} = k_x\hat{u}_x + k_y\hat{u}_y$, then the application of the ABC give rise to a reflected field having a wavenumber $\boldsymbol{k} = -k_x\hat{u}_x + k_y\hat{u}_y$. However, it should be noted that the incident field on the right-hand side boundary would admit two different values of k_y given by $\pm\sqrt{(k^2 - k_x^2}$. This is because of waves that have been reflected off the upper terminal boundary. Node B, or more precisely the numerical counterpart of node B, which comprises x_{11}, x_{12}, x_{13}, and B (see Fig. 9) now experiences waves that are reflected off node A. To node B (again, inclusive of the stencil), these waves are "incident" with $\boldsymbol{k} = -k_x\hat{u}_x \pm |k_y|\hat{u}_y$, which in effect resemble waves incident upon the upper terminal boundary from outside. This can lead to an uncontrollable growth in the field, or instability, since the ABC was not designed to absorb such waves.

Viewed from another different, yet, coherent perspective, the artificial reflection caused by the reflection from node A can be considered as an energy source as far as node B is concerned. To make this clear, let us consider once again points A and B in Fig. 9. These two points are located at two different physical locations. However, when the discretized ABC is applied at each of these two points, their stencils overlap, thus creating numerical points within the stencil that are supposed to be analytically unique. Let us assume that the ABC is first applied at A. After at least one time step from the time the field arrives at A, an artificial reflection is introduced at node x_{11} (see Fig. 9). Since this field appears at node x_{11} without passing through any of the earlier nodes of the stencil of B (x_{12} and x_{13}), it is effectively an independent source of energy as seen by node B. In fact the field experienced by B can no longer be characterized by incoming and outgoing waves only, but also by an additional source term as

$$u(x) = a^+ e^{-jk_y y + \omega t} + a^- e^{jk_y y + \omega t} + b(t). \tag{6}$$

Here $b(t)$ is a function of time that represents the appearance of a field that is not governed by the homogeneous wave equation.

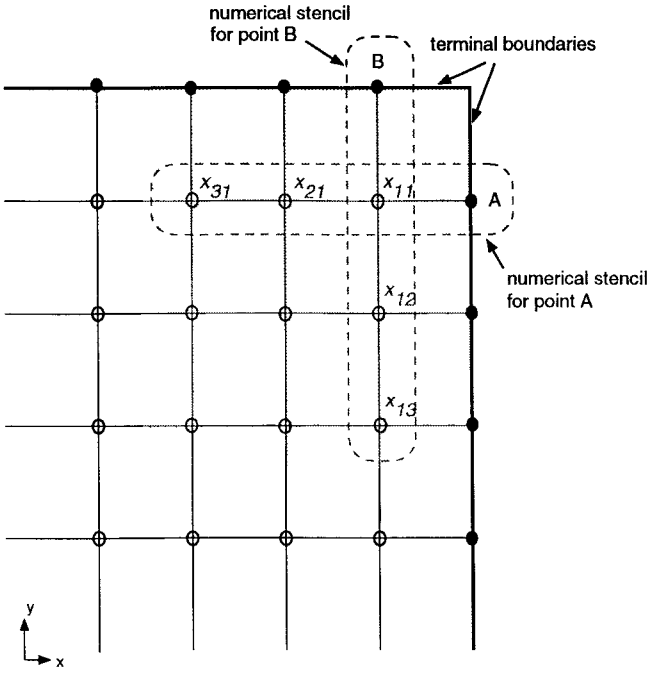

Fig. 9. Corner region showing the overlap between the stencils needed to descretize the boundary condition on boundaries A and B.

A source within the stencil of the boundary condition cannot be satisfied by the boundary condition since it violates the boundary condition, which is homogeneous, having the form $B\{u\} = 0$ instead of the inhomogeneous boundary condition $B\{u\} + a = 0$, where a is a constant. It is clear at this point that an inhomogeneous boundary condition is a good candidate for canceling the effect of $b(t)$. However, considering the fact that $b(t)$ is a function that cannot be predicted in advance, inhomogeneous boundary conditions are very restrictive; and it is conjectured that they do not have practical applications in FDTD simulations except in very limited applications where the physical source of excitation lies outside the computational domain [20].

In light of the above discussion, a question arises: If the overlap of ABC stencils in the corner region creates an incompatibility, then why would lower order ABC's such as Higdon's and Liao's second-order operators exhibit stable behavior? A careful look at Higdon and Liao second-order ABC's reveals that they too exhibit a degree of instability, however, much less pronounced than that exhibited by higher order operators. To show this, we reconsider the domain shown in Fig. 4, but without the conducting plates. In Fig. 10 we show the solution due to the application of Higdon's second-order ABC without stabilizing parameters. For all practical applications, such instability is of very little consequence (the maximum signal level in Fig. 10 is 10^{-5}), however, its existence is predicted from the analysis given above.

V. Summary

In this paper, we presented an analysis of the cause and mechanism behind a type of instability that arises when using the FDTD method to solve open-region radiation problems. It was shown through an empirical study that when using

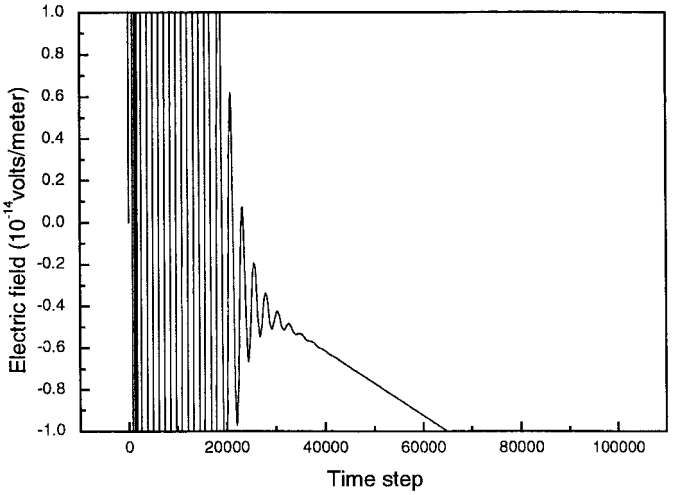

Fig. 10. Instability caused by Higdon second-order ABC.

a Cartesian mesh, instabilities arise due to corner regions, which are viewed as an artifact of the Cartesian computational domain. These incompatibilities are a direct consequence of the finite difference approximation used to transform the analytical equations into algebraic relations. It was shown that isolation of the corner region eliminates this dominant type of instability. As a consequence, we have identified an important class of FDTD applications that do not involve corner regions. This class of problems allows the application of higher-order ABC's that were typically considered unfit because of perceived instability potential.

Finally, it is hoped that identification of the cause of instability can lead to the construction of stable FDTD schemes employing rectangular mesh.

REFERENCES

[1] A. Sadigh and E. Arvas, "Treating the instabilities in marching-on-in-time method from a different perspective," *IEEE Trans. Antennas Propagat.*, vol. 41, Dec. 1993.

[2] S. D. Gedney and U. Navsariwala, "An unconditionally stable finite element time-domain solution of the vector wave equation," *IEEE Microwave Guided Wave Lett.*, vol. 5, pp. 332–334, Oct. 1995.

[3] J.-P. Berenger, "A perfectly matched layer for the absorption of electromagnetic waves," *J. Comput. Phys.*, vol. 114, pp. 185–200, 1994.

[4] S. Abarbanel and D. Gottlieb, "A mathematical analysis of the PML method," *J. Comput. Phys.*, vol. 134, pp. 357–363, 1997.

[5] Bayliss and E. Turkel, "Radiation boundary conditions for wave-like equations," *Comm. Pure Appl. Maths.*, vol. 23, pp. 707–725, 1980.

[6] B. Engquist and A. Majda, "Absorbing boundary conditions for the numerical simulation of waves," *Math. Comput.*, vol. 31, no. 139, pp. 629–651, July 1977.

[7] R. L. Higdon, "Absorbing boundary conditions for difference approximations to the multidimensional wave equation," *Math. Comput.*, vol. 47, no. 176, pp. 437–459, Oct. 1986.

[8] ———, "Radiation boundary conditions for elastic wave propagation," *SIAM J. Numer. Anal.*, vol. 27, no. 4, pp. 831–870, Aug. 1990.

[9] O. M. Ramahi, A. Khebir, and R. Mittra, "Numerically derived absorbing boundary conditionfor the solution of open region scattering problems," *IEEE Trans. Antennas Propagat.*, vol. 39, pp. 350–353, Mar. 1991.

[10] B. Stupfel and R. Mittra, "Numerical absorbing boundary conditions for the scalar and vector wave equations," *IEEE Trans. Antennas Propagat.*, vol. 44, pp. 1015–1022, July 1996.

[11] O. M. Ramahi, "Complementary boundary operators for wave propagation problems," *J. Comput. Phys.*, vol. 133, pp. 113–128, 1997.

[12] ———, "Concurrent implementation of the complementary operators method in 2D space," *IEEE Microwave Guided Wave Lett.*, vol. 7, pp. 165–167, June 1997.

[13] R. L. Wagner and W. C. Chew, "An analysis of Liao's absorbing boundary condition," *J. Electromagn. Waves Applicat.*, vol. 9, nos. 7/8, pp. 993–1009, 1995.

[14] O. M. Ramahi, "Stable FDTD solutions with higher-order absorbing boundary conditions," *Microwave Opt. Technol. Lett.*, vol. 15, no. 3, pp. 132–134, June 1997.

[15] I. Harari, "Accurate finite difference methods of time-harmonic wave propagation," *J. Comput. Phys.*, vol. 119, pp. 252–270, 1995.

[16] F. Moglie, S. Amara, T. Rozzi, and E. Martelli, "De-embedding correction for imperfect absorbing boundary conditions," *IEEE Microwave Guided Wave Lett.*, vol. 6, pp. 37–39, Jan. 1996.

[17] M. A. Schamberger, S. Kosanovich, and R. Mittra, "Parameter extraction and correction for transmission lines and discontinuities using the finite-difference time-domain method," *IEEE Trans. Microwave Theory Tech.*, vol. 44, pp. 919–925, June 1996.

[18] R. Janaswamy and Y. Liu, "An un-staggered collocated finite-difference scheme for solving time-domain Maxwell's equations in curvilinear coordinates," *IEEE Trans. Antennas Propagat.*, vol. 45, pp. 1584–1591, Nov. 1997.

[19] O. M. Ramahi, "The concurrent complementary operators method for FDTD mesh truncation," *IEEE Trans. Antennas Propagat.*, vol. 46, Oct. 1998.

[20] B. Gustafsson, "Inhomogeneous conditions at open boundaries for wave propagation problems," *Appl. Numer. Math.*, vol. 4, pp. 3–19, 1988.

Omar M. Ramahi (S'86–M'90) for photograph and biography, see p. 1482 of the October 1988 issue of this TRANSACTIONS.